NASA Technical Memorandum 81474

PREDICTING THE TIME-TEMPERATURE DEPENDENT AXIAL FAILURE OF B/Al COMPOSITES

James A. DiCarlo
Lewis Research Center
Cleveland, Ohio 44135

Presented at the
Symposium on Failure Modes in Composites
sponsored by the Metallurgical Society
of the American Institute of Mining, Metallurgical,
and Petroleum Engineers
Las Vegas, Nevada, February 25-26, 1980

PREDICTING THE TIME-TEMPERATURE DEPENDENT AXIAL FAILURE OF B/Al COMPOSITES

By James A. DiCarlo

National Aeronautics and Space Administration
Lewis Research Center
Cleveland, Ohio

INTRODUCTION

The ability to predict the failure modes of structural materials under various environmental conditions has both a practical and fundamental significance. On the practical side, the predictive theory and associated equations will allow the design engineer to estimate structural failure for conditions not covered in available test data. On the fundamental side, verification of the predictive theory by comparison with experimental data will confirm the mechanistic models employed to derive the theory. Such confirmation not only may allow future theoretical modifications which yield a more accurate predictive ability but also may lead to the development of practical techniques for improving structural performance.

The objective of this paper is to demonstrate that predictive equations can be developed that adequately describe the effects of time, temperature, and stress on the axial failure modes of B/Al composites. For many metal matrix composite systems the reinforcing fibers deform elastically so that time-temperature effects arise mainly from the mechanical properties of the matrix. However, for B/Al composites, both the matrix and fiber make major contributions to the time and temperature dependence of composite failure. This is due to the fact that in contrast to other ceramic fibers such as silicon carbide and alumina, boron fibers display a low temperature creep which has a significant effect on fiber fracture. For this reason the approach taken in this paper will be to first investigate boron fiber creep

and fracture data in order to establish a model and equations that accurately describe the axial failure modes of as-produced fibers. Once this is accomplished, composite data will be examined to determine how these equations might be modified to describe fiber creep and fracture within B/6061 Al composites. As part of this examination, a general metal matrix composite fracture theory will be developed based on the primary fiber amd matrix mechanisms which contribute to time and temperature-dependent axial composite failure.

PROCEDURE

Background

The low temperature deformation of a boron fiber has been observed to be characteristically anelastic [1,2,3]. That is, in a creep test upon application of a constant tensile stress σ at time $t = 0$, the total strain ε in the fiber increases with time t and temperature T according to

$$\varepsilon(t,T,\sigma) = \varepsilon_e(T,\sigma) + \varepsilon_a(t,T,\sigma) \qquad (1)$$

Here $\varepsilon_e = \sigma/E\ (T)$ is the time-independent elastic strain which depends on T only through the elastic Young's modulus E. The anelastic creep strain ε_a is zero at $t = 0$ but increases with time, temperature, and stress. No evidence of plastic strain or strains other than elastic and anelastic has been found in boron fiber deformation for temperatures up to 800° C. Three properties which characterize ε_a and distinguish it from plastic strain are:

I. Linearity: ε_a is directly proportional to σ.

II. Equilibrium: After passage of sufficient time, ε_a reaches or relaxes to a unique equilibrium value.

III. Recoverability: Upon removal of σ, the developed ε_a completely disappears at a rate which is time and temperature dependent.

Because of property I it is convenient to introduce a stress-independent anelastic strain function A defined by

$$A(t,T) = (\epsilon/\epsilon_e) = 1 + (\epsilon_a/\epsilon_e) \ . \qquad (2)$$

A = 1 for pure elastic behavior, and A > 1 for anelastic behavior. With this definition for A, Eq. (1) can be rewritten as

$$\epsilon(t,T,\sigma) = [\sigma/E(T)]A(t,T) \qquad (3)$$

which is simply Hooke's law multiplied by the time-temperature dependent factor A. Clearly, to understand and predict the effects of anelastic deformation on the failure modes of boron fibers and B/Al composites, one must have accurate knowledge of the boron A function. In this paper the results of various deformation experiments will presented in which Eqs. (2) and (3) were employed to calculate the A functions for as-produced boron fibers and for fibers within B/Al composites.

Deformation tests

The primary experiments employed to determine the A function for as-produced boron fibers were low-stress flexural stress relaxation (FSR) and flexural internal friction (FIF) tests performed at various temperatures up to 800° C. Details of the test apparatus and applicable deformation theories are described elsewhere [1]. For the FSR tests, anelastic creep strains were allowed to develop for one hour, whereas for the FIF tests, creep occurred only in a time span of one vibration period which was typically of the order of one millisecond. This large difference in test time couple with anelasticity theory permitted accurate extrapolation of the A function for time-temperature conditions not covered by the tests.

As predicted by anelasticity property I, the A functions measured by the low-stress flexural tests were found to be independent of the applied stress.

However, when the FSR tests were conducted at stress levels above 50 ksi, (0.3 GN/m^2) an unexpected stress dependence for the A function was observed. To study this effect in greater detail, two types of high stress tensile experiments were performed: room temperature elongation experiments [4] at stress levels of about 400 ksi (2.8 GN/m^2), and stress rupture experiments on etched boron fibers (1) at temperatures from 200 to 1000° C and at stress levels between 200 and 800 ksi (1.4 and 5.6 GN/m^2). Since the latter experiments have a direct bearing on a predictive fracture model for boron fibers, the details of the deformation theory involved in its interpretation will be discussed here.

After slightly etching 203 μm boron on tungsten fibers, Smith [5] observed that essentially all cases of fiber fracture could be explained by crack initiation within the region of the tungsten boride core. This result suggests a "composite fiber" fracture model in which an etched boron on tungsten fiber fractures whenever the total axial strain of the boron anelastic sheath becomes equal to the core fracture strain. By assuming a brittle elastic core with a fracture strain independent of time and temperature, one can then use Eq. (3) to express this model in the following form:

$$\bar{\varepsilon}_u = [\bar{\sigma}_u(t,T)/E(T)]A(t,T) = \text{CONSTANT} \qquad (4)$$

Here $\bar{\varepsilon}_u$ is the average (ultimate) fracture strain of the etched fiber, and $\bar{\sigma}_u$ is the average (ultimate) fracture stress required to obtain $\bar{\varepsilon}_u$. In the stress rupture tests, $\bar{\sigma}_u(t,T)$ were measured for various times and temperatures. These data plus room temperature $\bar{\varepsilon}_u$ data were then inserted into Eq. (4) to determine the A function at the $\bar{\sigma}_u$ stress level.

To determine the A function for fibers within B/Al composites, it was necessary to perform a composite test in which essentially all deformation is fiber controlled. One test that fulfills this requirement is the internal

friction or damping test conducted on B/Al composites which have been annealed near 400^{o} C. The experimental and theoretical details of this test are described elsewhere [6]. The annealing treatment essentially eliminates dislocation damping within the aluminum matrix, leaving the fibers as the only source of composite damping [7]. Application of the rule-of-mixtures to axial temperature-dependent damping data for undirectional B/Al composites allowed accurate calculations of fiber damping as a function of temperature. As previously described for the FIF data [1], these fiber damping results were then used as deformation data to calculate the A function for fibers within B/Al composites. The stress levels of the composite damping test varied between 0.01 and 1 ksi (0.07 and 7 MN/m^2). In this range no stress effects on fiber damping were observed, indicating a true stress independence for the A function up to at least 1 ksi.

Specimens

The primary specimens employed for the single-fiber tests were 203 μm (8 mil) and 142 μm (5.6 mil) boron on tungsten fibers supplied by Avco Specialty Materials Division. During the chemical vapor deposition of the boron sheath, the original 13 μm tungsten substrate became completely borided to form a 17 μm diameter core region.

Because fiber coatings may have an affect on the fiber anelasticity, 142 μm boron fibers coated with a 1.5 μm thick silicon carbide layer were also examined. These fibers which also contained the 17 μm tungsten-boride core were supplied by Composite Technology Inc. under the tradename "Borsic".

The unidirectional B/Al composite specimens employed for the damping experiments contained normally 50 volume percent boron or Borsic fiber in a 6061 Al matrix. The specimens reinforced by 203 μm boron fibers were fabricated by TRW whereas those reinforced by the Borsic fibers were fabricated by

Avco. Typical fabrication techniques involving diffusion bonding near 500° C were employed for both composite types.

RESULTS AND DISCUSSION

As-Produced Fibers

Fiber creep. - In previous work (1) it was determined that anelastic creep in boron fibers is a thermally-activated process. As such, the time and temperature conditions required to produce a certain anelastic strain ϵ_a are not independent variables. That is, fixing the test temperature fixes the deformation time at which the given strain will be reached. The results of the low-stress FSR and FIF test indicated that for boron fibers, the relationship between the time and temperature variables was best expressed in terms of a q parameter given by

$$q = (\ln t + 33.7)\, T(10^{-3}). \tag{5}$$

Here t is deformation time in seconds and T is test temperature in degrees Kelvin. Thus, ϵ_a and the anelastic function A depend only on the one variable q rather than the two variables t and T. This result greatly simplified the experimental procedures required to determine the A function. For example, since q is weakly dependent on time ($\ln t$) and directly proportional to temperature, deformation tests were typically conducted by holding the deformation time constant and measuring the development of anelastic creep strain as a function of test temperature. The deformation strains and Eqs. (2) and (3) were then used to calculate $A(q)$ at the q value corresponding to the particular time-temperature test conditions.

The $A(q)$ results from the low-stress flexural tests on as-produced fibers are shown as curve A_L in Fig. 1. The subscript L refers to the fact that the measurements were made at low stresses below 50 ksi (0.3 GN/m^2) where

A(q) was observed to be stress independent. Actual data points are not indicated because they have negligible error and were measured almost continuously ($\Delta q \simeq 0.3$ K). To put these results in perspective, a 60 sec test at room temperature corresponds to a q value of 11 K whereas a 1000 hr test at 300° C yields a q value of 28 K. Since $A_L \simeq 1$ for q values less than 15 K, it follows that at low stresses and short times, boron fibers deform essentially elastically at room temperature and below. However, at longer times or higher temperatures, these fibers will display anelastic creep, even at very low stress.

As previously discussed, raising the stress level above 50 ksi (0.3 GN/m^2) produced an unexpected increase in the A function. To study this effect, tensile elongation and fracture tests were conducted on single fibers. In Fig. 2 the A function results from the tensile and flexural tests are plotted as a function of stress for q values of 11, 20, and 29 K. For tests of one minute duration, these values roughly correspond to test temperatures of 20°, 250°, and 500° C. Although the stress effect data are limited, the Fig. 2 curves were drawn assuming a discontinuous behavior for the boron fiber A function. That is, as stress increases the, A function remains constant at the A_L level until at some transition stress σ^* where it rather abruptly increases to a constant A_H level as measured by the tensile fracture tests on etched fibers. The subscript H refers to the "high" stress level (>400 ksi (2.8 GN/m^2)) of these measurements (1). The q dependence of the A_H function is shown in Fig. 1. The large error bars for the A_H data points are due primarily to a coefficient of variability of ~5 percent in the fracture stress data.

Although it is not obvious that the Fig. 2 stress effect data support the assumption of an abrupt increase in A from one level to another, there does

exist some indirect evidence for such behavior. For example, in previous work it was shown that boron fiber anelasticity could be explained by grain boundary type sliding of small substructural boron units [2,4]. Based on this microstructural model, the maximum A function to be expected for boron fibers is given approximately by the A_H curve of Fig. 1. The fact that A_L is less that A_H suggests that at low stress all boron units cannot participate in creep, due possibly to the existence of some unknown internal "locking" mechanism. The stress-induced increase from A_L to A_H indicates that high stress can unlock the immobilized units, giving rise to maximum anelastic creep. If the locking mechanisms are all of one type, one might expect that the unlocking should occur over a narrow stress range. Experimental support for this may be found in the boron fiber torsional damping data of Firle [8] who observed that as shear stress is increased, fiber damping remains constant until some high shear stress level at which it increases rather abruptly over a small stress range. Thus, the assumption is made that A_L and A_H are constant over certain stress regimes and that the transition from A_L to A_H occurs abruptly at σ^*. As indicated by the Fig. 2 curves, σ^* decreases with increasing q or temperature, suggesting that the unlocking mechanism is thermally activated.

Summarizing the practical aspects of the above results, one can now predict creep of as-produced boron fibers by employing the following equation:

$$\epsilon(t,T,\sigma) = [\sigma/E(T)]A_\sigma(q) \qquad (6)$$

where $A_\sigma = A_L$ for $\sigma < \sigma^*$ and $A_\sigma = A_H$ for $\sigma > \sigma^*$. The q parameter is given by Eq. (5) and $\sigma^*(q)$ can be estimated from the Fig. 2 results. Accurate data for $E(T)$ were measured during the single fiber damping tests (1,4). These data are shown in Fig. 3 in terms of the ratio $E/E(20^\circ\ C)$ where $E(20^\circ\ C) = 60.5\times10^6$ psi (418 GN/m^2).

It should be noted that Eq. (6) describes the total deformation strain which includes both the elastic and anelastic strain components. One can calculate the anelastic creep strain ϵ_a simply by replacing A_σ by $(A_\sigma - 1)$ in Eq. (6). However in any practical fiber creep test, it would be very difficult to observe ϵ_a directly since like the elastic strain it develops linearly with stress and also begins to recover immediately upon stress removal. For this reason, total deformation strain is considered to be a more practical parameter for understanding and describing boron fiber creep. One final design point is that although considerations of stress effects on A_σ may be important in some situations, one could in many circumstances neglect the stress effects and design for the upper limit boron fiber creep by simply employing A_H in Eq. (6).

Fiber fracture. - Smith has observed that the two primary flaw sites responsible for crack propagation in commercially-produced boron fibers are located within the tungsten boride core and on the fiber surface [5]. By slightly etching the as-produced fibers, he was able to remove the surface flaws and thus observe only core flaw-initiated fiber fracture. As described earlier, one can utilize this fact to develop a "composite fiber" fracture model for calculating the high stress A_H from fracture stress data on slightly etched as-produced fibers. The basic equation for this model is Eq. (4) in which it is assumed fiber fracture occurs at the core fracture strain which is time and temperature independent. Since fracture stress data were employed to determine A_H, it follows that Eq. (4) can be transposed to predict $\bar{\sigma}_u$ as a function of time and temperature. That is, the average fracture stress of an etched fiber (core controlled fracture) can be calculated from the equation

$$\bar{\sigma}_u(q) = \bar{\sigma}_u(q_o) \frac{E(T)}{E(T_o)} \quad \frac{A_H(q_o)}{A_H(q)} \tag{7}$$

Here $\overline{\sigma}_u(q_o)$ is the average fracture stress measured at some reference q_o condition, such as, a short-time tensile test ($t_o \simeq 60$ sec) at room temperature ($T_o = 293$ K). Although $A_H(q)$ was determined from short-time fracture test data, it should be realized that theoretically Eq. (7) can be generalized through the q parameter to predict core-initiated fracture during other time-dependent tests such as impact and long-time stress rupture. At the present time, however, no data exist to confirm the validity of Eq. (7) for other than the short-time tensile test.

The derivation of Eq. (7) was simplified by the fact that the etched fiber could be treated as a two component composite in which the outer sheath component fractures whenever the inner core component reaches its fracture strain. This composite model may not be valid, however, when the source of fiber fracture are flaws on the fiber surface. In most as-produced commercial boron fibers, Smith [5] has observed only surface flaw and core-initiated fractures. He found that the two flaw types can be practically distinguished by the fact that core-initiated fractures generally produce strength values greater than 600 ksi (4.1 GN/m^2) whereas surface flaw-initiated fractures produce strength values less than 500 kis (3.4 GN/m^2). Since commercial boron fiber spools are generally quoted at average strengths of 500 ksi, it follows that surface flaws do exist in these fibers. Thus, the question arises whether Eq. (7) can be utilized to predict fracture stress of unetched as-produced fibers.

This question was examined empirically by plotting in Fig. 4 the short-time temperature-dependent fracture stress data of Veltri and Galasso [9] for unetched as-produced boron fibers. To better compare these data with the theoretical predictions of Eq. (7), the fracture stress values were normalized by

dividing $\bar{\sigma}_u$ by the room temperature value, $\bar{\sigma}_u(q_0) = 500$ ksi (3.4 GN/m^2). The range of the theoretical estimates based on Eq. (7) and the errors in A_H (cf. Fig. 1) are shown by the dashed lines. Comparing these with the experimental data, one finds that although surface flaws were most probably controlling fiber fracture, it does appear that Eq. (7) predicts quite well the fracture stress of both etched and unetched as-produced fibers. From this result it follows that Eq. (7) can be employed as the general equation for predicting boron fiber fracture stress regardless of the flaw type responsible for fracture initiation. However, it should be realized that anelastic creep effects on fiber fracture are contained in the A_H function used in Eq. (7). Thus, in light of the stress effect curves of Fig. 2, one should replace A_H by A_L if fiber flaws should initiate fracture at stress levels below the transition stress σ^*.

B/Al Composites

Fiber creep. - The anelastic A function for boron fibers within B/6061 Al composites was determined from composite damping data [6]. The results are shown in Fig. 5 as curve A_L^{II}. The subscript L again refers to the fact that low fiber stresses (<1 ksi (7 MN/m^2)) were used for these measurements. The superscript II is used to distinguish the results for fibers within B/Al composites from the as-produced fiber results which are now labeled with the superscript I.

Comparing the A_L^{II} curve with the as-produced A_L^{I} curve, which is also shown in Fig. 5, one observes that the anelastic creep of the as-produced boron fibers is measurably reduced within B/Al composites. Obviously a microstructural change must have occurred in the fiber at some time during composite fabrication. Since the most adverse environmental conditions existed during high temperature diffusion bonding of the composite

specimen, the microstructural change most probably occurred during this stage when the boron fibers reacted with the aluminum matrix to form the interfacial bond required for mechanical load transfer. In support of this surface reaction effect on the A function, it was found [7] that Borsic fibers in both the as-produced and composite conditions possess low stress A functions equivalent to the A_L^{II} result of Fig. 5. Thus, on the basic level, the boron fiber microstructure responsible for its bulk anelastic deformation character can be measurably affected by surface reactions either with matrices or with fiber coatings. In terms of the boron unit sliding model, it would appear that at the high temperatures of the surface reactions, diffusional processes occur within the fiber which increase the number of immobilized boron units.

Although A_L^{II} can now be inserted into Eq. (6) to accurately predict low-stress boron and Borsic creep in B/Al composites, the upper stress limit σ^* at which it can no longer be validly employed remains undetermined. As with the as-produced single fibers, high stress deformation experiments are required from which A^{II} versus stress data can be determined. These experiments could be performed either on single fibers extracted from B/Al composites or on unidirectional B/Al composites in which the fiber contributions can be easily and accurately measured. One obvious method of maximizing fiber effects and minimizing matrix effects in composites would be to study specimens with fiber volume fractions of 50 percent or greater. It should be mentioned that high stress creep data for 50 fiber volume percent B/Al composites do exist in the literature [10]. Attempts to employ these data for extracting high stress A^{II} curves were not very fruitful, primarily due to the existence of unknown matrix stress relaxation effects on total composite creep [11]. However, although composite creep data were not

useful, it was found that a theoretical study of composite fracture stress versus temperature data could not only shed light on high stress effects on fiber creep but also yield equations for predicting time-temperature effects on B/Al fracture. The theory and results of this study will now be discussed.

Composite fracture. - Having established that the A_H function is the appropriate function for predicting high stress fracture of single as-produced fibers, the first question to be answered is whether this function can be used also to predict the high stress creep and fracture of boron fibers within B/Al composites. To examine this question, a literature search was conducted for short-time fracture stress versus temperature data for B/6061 Al composites. In order to minimize matrix loading effects, the search was confined only to composites with nominally 50 percent fiber volume fraction. Summary plots of the literature data which fit this requirement are shown in Fig. 6. Although the tensile strengths vary in magnitude from one source to another, one can notice definite trends in the temperature-dependent behavior. For example, below 200^{o} C the data from all sources indicate essentially no dependence on temperature. Above 200^{o} C the strength data fall off reaching about 80 percent of the room temperature value near 300^{o} C.

Regarding fracture of fibers within B/Al composites, one might as a first approximation neglect matrix contributions and assume that the composite stress should drop off at least as rapidly as the fracture stress for single as-produced boron fibers. Examining the experimental results of Fig. 4, it is seen that single as-produced fibers fall off to 80 percent of $\bar{\sigma}_u(q_o)$ near 150^{o} C, a much faster dropoff than the composite. Thus, from a practical point of view it appears that the Veltri and Galasso data for as-produced fibers cannot be used to understand and predict the temperature dependence of composite strength. From an analytical point of view, one must conclude that

the insertion of the A_H in the fiber fracture theory of Eq. (7) will not explain the Fig. 6 composite data. Since the A_L results of Fig. 5 indicate that boron fibers still creep within B/Al composites, the problem of predicting the effects of time and temperature on B/Al axial fracture thus becomes one of not only accounting for matrix plasticity but also of determining the appropriate A function for high stress creep and fracture of the fibers after composite fabrication.

To solve this problem, a theoretical analysis was made of the major factors which affect the temperature-dependent behavior of the fracture stress of metal matrix composites in general and B/6061 Al composites in particular. The axial fracture model chosen is that developed by Rosen [12] in which the fracture modes of fibers within an unidirectional composite are controlled by the fracture of fiber bundles. That is, the composite or fiber bundle completely fails when enough fiber breaks occur so that the load carried by the remaining intact fibers exceeds their strength capability. Due to a distribution in fiber strengths, the weak fibers fracture first leaving the stronger fibers to carry the load. Common practice is to describe the distribution in fiber strengths according to a Weibull distribution [13]. In this case, the average fiber strength $\bar{\sigma}_{uf}$ and the average fiber bundle strength $\bar{\sigma}_{bf}$ are given by

$$\bar{\sigma}_{uf} = \sigma_o \left[\frac{L_s}{d}\right]^{-1/\omega} \Gamma\left(\frac{\omega + 1}{\omega}\right) \tag{8}$$

and

$$\bar{\sigma}_{bf} = \sigma_o \left[\frac{e\omega L_b}{d}\right]^{-1/\omega} \tag{9}$$

Here σ_o is the Weibull distribution scale factor, ω is the Weibull shape factor which describes the scatter in strength values, Γ is the tabulated

gamma function, e is the natural base constant, d is the fiber diameter, and L_s and L_b are the test gage lengths of the single fiber and the fiber bundle, respectively. Typically $\omega > 1$, so that $\bar{\sigma}_{bf}$ decreases as the bundle length increases.

When a fiber breaks in a metal matrix composite, the matrix by virtue of its plastic character localizes the loss of load carrying ability of the broken fiber. That is, at an axial distance $\delta/2$ on either side of the break, the stress in the broken fiber returns to the average stress of all the intact fibers. Because of the existence of this "ineffective" length δ, Rosen considers the composite to be made of a series of independent fiber bundles each of length δ. As such, total fracture of the composite occurs whenever any one of these short length bundles fail. If one assumes perfectly plastic behavior for the matrix (no workhardening effects), the length δ of the bundles can be calculated from

$$\delta = \sigma d/2\tau_m \tag{10}$$

where $\sigma = \bar{\sigma}_{bf}$ is the stress in the fibers at composite fracture and τ_m is the shear strength of the matrix. Since τ_m decreases with temperature, it follows that δ will increase, giving rise by Eq. (9) to a reduction in $\bar{\sigma}_{bf}$ with temperature.

To express the total stress level at which a metal matrix composite will fracture, one can employ the above concepts to write the following rule-of-mixtures equation for the average (ultimate) tensile strength of the composite

$$\bar{\sigma}_{uc} = v_f \, \bar{\sigma}_{bf} \, (\delta) + v_m \, \sigma_{ym}(T) \tag{11}$$

Here v_f and v_m are the volume fraction of the fiber and matrix, respectively, and σ_{ym} is the tensile yield strength of the matrix. Eq. (11) neglects stress concentration effects of broken fibers on nearby fibers. It also neglects residual stress effects on the fibers due to cooling the composite from fabrication temperature. For soft matrices such as aluminum these effects are small and also tend to oppose each other as temperature is varied. For calculating the temperature dependence of $\bar{\sigma}_{uc}$ it is convenient to normalize each stress term in Eq. (11) by dividing by its value for a short-time tensile test at room temperature. The following R parameters are thus defined:

$$R_{uc} = \bar{\sigma}_{uc}(q)/\bar{\sigma}_{uc}(q_o) \tag{12}$$

$$R_{bf} = \bar{\sigma}_{bf}(q)/\bar{\sigma}_{bf}(q_o) \tag{13}$$

$$R_{ym} = \sigma_{ym}(T)/\sigma_{ym}(T_o) \tag{14}$$

In anticipation of applying these equations to B/Al composite behavior, the temperature variable T was replaced, where appropriate, by the more general q variable. Reference conditions (q_o and T_o) are taken as a short-time ($t_o \simeq 60$ sec) tensile test at room temperature ($T_o \simeq 293^o$ K). Inserting Eqs. (12), (13), and (14) into Eq. (11) one obtains

$$R_{uc} = (R_{bf} + \beta R_{ym})/(1 + \beta) \tag{15}$$

where the constant $\beta = v_m \sigma_{ym}(T_o)/v_f \bar{\sigma}_{bf}(q_o)$. Thus, to predict composite fracture stress $\bar{\sigma}_{uc}(q)$, one simply needs a theoretical formula for R_{bf} plus experimental information for $\bar{\sigma}_{uc}(q_o)$ and $R_{ym}(T)$.

To derive R_{bf} one can utilize Eq. (9) to write

$$R_{bf} = \frac{\sigma_o(q)}{\sigma_o(q_o)} \left[\frac{\delta(T)}{\delta(T_o)}\right]^{-1/\omega} \tag{16}$$

Here it is assumed that the flaw distribution as measured by ω does not change during the test. Also, to include fiber creep effects, a q dependence has been assigned to σ_o since by Eq. (8), σ_o is the only term responsible for a change in fiber strength with temperature. Assuming matrix shear strength τ_m is directly proportional to matrix yield strength σ_{ym}, one finds from Eq. (10) that

$$\delta(T)/\delta(T_o) = R_{bf}/R_{ym} \tag{17}$$

By inserting this result into Eq. (16) and manipulating, it follows that

$$R_{bf} = \left[\frac{\sigma_o(q)}{\sigma_o(q_o)}\right]^{\omega/(1+\omega)} \left[R_{ym}\right]^{1/(1+\omega)} \tag{18}$$

Thus, under the assumptions stated above, one should now be able to employ Eqs. (15) and (18) to predict the time-temperature dependent fracture stress of metal matrix composites. For those composites reinforced by boron fibers, both terms on the right hand side of Eq. (18) must be considered. However, for those composites reinforced by elastic fibers, $\sigma_o(q) = \sigma_o(q_o)$ so that only the second matrix-related term need be considered.

To determine the high stress A function for boron fibers in B/Al composites, Eqs. (15) and (18) were applied to the experimental strength data of Fig. 6. It was assumed that the temperature dependence of R_{ym} for the 6061 aluminum matrix followed that measured by Prewo and Kreider [14] for the transverse tensile strength of as-fabricated B/6061 composites. Their results which are plotted in Fig. 6 show a drop in transverse strength from 20 ksi (138 MN/m^2) at room temperature to an extrapolated value of 3 ksi (21 MN/m^2) at 370° C [21]. Assuming a room temperature matrix shear strength of 14 ksi (97 MN/m^2) [15] and a 5.6 mil (142 μm) diameter fiber whose

strength falls off by 70 percent at 370° C, it follows from Eq. (10) that the ineffective length δ increases from 0.1 to 0.5 inch (2.5 to 12 mm) between 20° and 370° C. To compare the Fig. 6 strength data with theory, each set of data was normalized by dividing by their room temperature values and the best fit R_{uc} for all sets was calculated. The best fit result is shown by the dashed curve of Fig. 7.

Regarding values for the parameters in the theoretical equations, σ_{bf} and σ_{ym} at room temperature were assumed to be 400 and 8 ksi (2.8 and 0.06 GN/m^2) [14], so that $\beta = 0.02$ for 50 percent fiber content in as-fabricated 6061 Al. In examining the literature for information concerning the Weibull distribution of boron fibers removed from B/6061 Al composites, ω parameters were found which range between 8 and 12 with $\omega = 10$ as an average value [14,15,16). Since the boron fibers definitely show anelastic creep within the composites, the assumption was made that fiber fracture could be described by Eq. (7) with an appropriate A function. Thus, for Eq. (18), one can write

$$R_{bf} = \left[\frac{E(T)\ A(q_o)}{E(T_o)\ A(q)}\right]^{\omega/(1+\omega)} \left[R_{ym}\right]^{1/(1+\omega)} \qquad (19)$$

With $\omega = 10$, R_{bf} was inserted into Eq. (15) and R_{uc} was calculated for three different A functions: A = 1 which assumes strictly elastic fiber behavior (no creep), $A = A_H$ which assumes the as-produced high stress condition for the fibers, and $A = A_L^{II}$ which assumes that the low stress creep behavior does not change for fiber stresses up to ~400 ksi (2.8 GN/m^2).

The theoretical results for the three A functions are shown in Fig. 7. For elastic fiber behavior, curve A = 1 clearly shows that composite strength should fall off simply due to matrix effects in which temperature decreases τ_m and increases the ineffective length δ. If $\omega = \infty$, which implies constant strength fibers, Eq. (19) indicates that the matrix would have no

effect on fiber bundle strength. For the assumption of as-produced behavior, the A_H curve obviously drops off much too rapidly to explain the experimental data. This point was previously discussed in comparing the as-produced fiber data of Fig. 4 with the composite data of Fig. 6. Finally, it appears that the A_L^{II} curve gives the best fit to the fracture data. Thus it may be reasonable to assume that fiber creep within B/Al composites is governed by only the A_L^{II} function from zero to at least 400 ksi (2.8 GN/m^2). The shift from A_L to A_H observed for the as-produced fiber (cf. Fig. 2) apparently does not occur for the B/Al fibers. From a basic point of view one might interpret this as an additional effect of the boron-aluminum interfacial reaction in that besides decreasing the number of mobile boron units, it may also affect the internal locking mechanism in such a way as to increase σ^* to values greater than 400 ksi.

Summarizing the design aspects of the above discussion, it appears that for any fiber stress less that 400 ksi (2.8 GN/m^2), the A_L^{II} curve of Fig. 2 is the proper A function for describing boron and Borsic creep in B/6061 Al composites. Thus, Eq. (6) with $A_\sigma = A_L^{II}$ is the predictive equation for fiber creep. Regarding composite fracture, Eqs. (15) and (18) with $A = A_L^{II}$ and $\omega = 10$ give good estimates of B/6061 Al axial fracture strength as a function of temperature. However, because of the thermally-activated nature of boron creep, these equations can be generalized through the q parameter to also include test conditions in which time is the principal variable. For example, in an axial stress rupture test, one can assume $\beta R_{ym} = 0$ (due to rapid stress relaxation in the matrix) and write for the stress rupture strength

$$\bar{\sigma}_{uc}(q) = \bar{\sigma}_{uc}(q_1)\left[\frac{A(q_1)}{A(q)}\right]^{\omega/(1+\omega)} \tag{20}$$

Here $q \geq q_1$ and $\bar{\sigma}_{uc}(q_1)$ is the short-time composite strength at temperature T_1 which is held constant during the test. Since q develops with the log of time, $\bar{\sigma}_{uc}$ should show only a weak time dependence. Indeed, limited stress rupture data for B/Al composites confirm such a dependence [17].

The apparent confirmation of the mechanistic theory used to calculate composite fracture stress suggests possible methods of improving the creep and associated stress rupture characteristics of B/Al composites. For example, the fact that fiber creep is reduced by high temperature surface reactions with an SiC coating and a 6061 aluminum matrix suggests that perhaps other fiber secondary treatment processes exist which can either eliminate of drastically reduce anelastic creep in the as-produced boron fibers. These treatment processes, however, should have minimum adverse effects on the as-produced fiber flaw character or else the benefits gained by reducing creep could be lost by a degradation in fiber strength. Regarding the matrix shear strength effect on composite fracture, it follows from Eq. (18) that this effect can be minimized by narrowing the distribution in fiber strengths (larger ω). Since it is generally flaws within the interfacial surface phase that control fiber fracture in metal matrix composites, the largest ω values should result from those bonding conditions which produce the most uniform distribution of interfacial flaws. Thus, a good mechanical interfacial bond may not only produce a stronger composite at room temperature but also at higher temperatures where matrix shear strength falls off.

SUMMARY OF RESULTS AND CONCLUSIONS

Due to the linear stress dependence of anelastic strain, it is possible to write simple analytical equations for describing boron fiber creep and fracture as a function of time, temperature, and stress. The primary time-temperature dependent variable in these equations is an anelastic strain

function A. From analysis of single fiber deformation and fracture data, A functions for commercial boron fibers were determined. Thus, the creep strain and stress rupture strength of as-produced boron fibers can now be predicted.

Analysis of Borsic fiber and B/Al composite damping data indicates that the creep of SiC coated boron fibers and of boron fibers in B/Al composites is measurably less than the creep of as-produced boron fibers. The reduced A function characteristic of fiber creep in B/Al composites was determined. This function together with a general metal matrix composite fracture theory should now allow fairly good estimates of the effects of time and temperature on the axial failure modes of B/Al composites. Based on the mechanistic models employed in this composite fracture theory, itappears that a good interfacial fiber-matrix bond will not only maximize mechanical load transfer but also may reduce detrimental fiber and matrix effects on B/Al stress rupture properties.

NOMENCLATURE

$A: A_L, A_H$	Anelastic strain function: at low stress, at high stress
d	fiber diameter
E	fiber Young's modulus
L_s, L_b	gage length of single fibers and fiber bundle
q	time-temperature parameter
R_{bf}, R_{uc}, R_{ym}	ratio of test value to short-time value at room temperature for fiber bundle strength, composite tensile strength, and matrix yield strength
t	deformation time (sec)
T	test temperature (K)
v_f, v_m	volume fraction of fibers and matrix

β	ratio of matrix load to fiber load under short-time composite loading at room temperature
δ	"ineffective length" of fiber bundles in composites
ε:ε_e, ε_a	total fiber strain: elastic component, anelastic component
$\bar{\varepsilon}_u$	average (ultimate) fiber fracture strain
σ_o	Weibull distribution stress factor
σ^*	transition stress for change from A_L to A_H
$\bar{\sigma}_{uf}$	average (ultimate) fiber tensile strength
$\bar{\sigma}_{bf}$	average fiber bundle strength
$\bar{\sigma}_{uc}$	average (ultimate) composite tensile strength
σ_{ym}	tensile yield strength for matrix
τ_m	shear strength for matrix
ω	Weibull distribution shape factor

Superscripts

I;II	for as-produced fibers; for fibers within B/Al composites

REFERENCES

1. J. A. DiCarlo: "Time-Temperature-Stress Dependence of Boron Fiber Deformation," Composite Materials: Testing and Design (Fourth Conference), AASTM STP 617, pp. 443-465, American Society for Testing Materials, Philadelphia, 1977.

2. K. M. Prewo: "Anelastic Creep of Boron Fibers," J. Compos. Mater., 1974, vol. 8, pp. 411-414.

3. J. A. DiCarlo: "Anelastic Deformation of Boron Fibers," Scripta Met., 1976, vol. 10, pp. 115-119.

4. J. A. DiCarlo: "Mechanical and Physical Properties of Modern Boron Fibers," ICCM/2, Second International Conference on Composite Materials, pp. 520-538, The Metallurgical Society of AIME, New York, 1978.

5. R. J. Smith: "Changes in Boron Fiber Strength due to Surface Removal by NASA TN D-8219, Washington, D.C., 1976.

6. J. A. DiCarlo and J. E. Maisel: "Measurement of the Time-Temperature Dependent Dynamic Mechanical Properties of Boron/Aluminum Composites," Composite Materials: Testing and Design (Fifth Conference), ASTM STP 674, pp. 201-227, American Society for Testing Materials, Philadelphia, 1979.

7. J. A. DiCarlo and W. Williams: "Dynamic Modulus and Damping of Boron Silicon Carbide, and Alumina Fibers," NASA TM-81422 Washington, D.C., 1980.

8. T. E. Firle: "Amplitude Dependence of Internal Friction and Shear Modulus of Boron Fibers," J. Appl. Phys., 1968, vol. 39, pp. 2839-2845.

9. R. D. Veltri and F. S. Galasso: "High-Temperature Strength of Boron, Silicon Carbide, Stainless Steel, and Tungsten Fibers," J. Am. Ceram. Soc., 1971, vol. 54, pp. 319-320.

10. K. G. Kreider and K. M. Prewo: "Boron-Reinforced Aluminum," Composite Materials, K. G. Kreider, ed., Vol. 4, pp. 399-471, Academic Press, New York, 1974.

11. A. R. T. de Silva: "A Theoretical Analysis of Creep in Fibre Reinforced Composites," J. Mech. Phys. Solids, 1968, vol. 16, pp. 169-186.

12. B. W. Rosen: "Tensile Failure of Fibrous Composites," AIAA J., 1964, vol. 2, pp. 1985-1991.

13. H. T. Corten: "Micromechanics and Fracture Behavior of Composites," Modern Composite Materials, L. V. Broutman and R. H. Krock, eds., pp. 27-105, Addison-Wesley, Reading, Mass., 1967.

14. K. M. Prewo and K.G. Kreider: "High Strength Boron and Borsic Fiber Reinforced Aluminum Composites," J. Compos. Mater., 1972, vol. 6, pp. 338-357.

15. M. A. Wright and J. L. Wills: "The Tensile Failure Modes of Metal Matrix Composite Materials," J. Mech. Phys. Solids, 1974, vol. 22, pp. 161-175.

16. M. A. Wright and D. Welch: "Failure of Centre Notched Specimens of 6061 Aluminum Reinforced with Unidirectional Boron Fibers," Fibre Sci. Technol., 1978, vol. 11, pp. 447-461.

17. E. M. Breinan and K. G. Kreider: "Axial Creep and Stress-Rupture of B-Al Composites," Metall. Trans., 1970, vol. 1, pp. 93-104.

18. D. A. Meyn: "Effect of Temperature and Strain Rate on the Tensile Properties of Boron-Aluminum and Boron-Epoxy Composites," Composite Materials: Testing and Design (Third Conference), ASTM STP 546, pp. 225-236, American Society for Testing Materials, Philadelphia, 1974.

19. J. L. Christian and M. D. Campbell: "Mechanical and Physical Properties of Several Advanced Metal-Matrix Composite Materials," Cryogenic Engineering Conference, Advances in Cryogenic Engineering, Vol. 18, pp. 175-183, Plenum Press, New York, 1973.

20. I. J. Toth: Composite Materials: "Comparison of the Mechanical Behavior of Filamentary Reinforced Aluminum and Titanium Alloys," Testing and Design (Third Conference), ASTM STP 546, pp. 542-560, American Society for Testing Materials, Philadelphia, 1974.

21. Metals Handbook, Vol. 1, p. 946, American Society of Metals, Metals Park, Ohio, 1961.

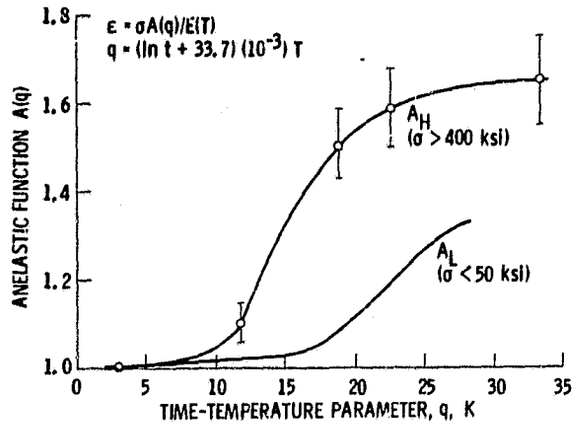

Figure 1. - The anelastic strain functions for as-produced boron fibers.

CS-80-928

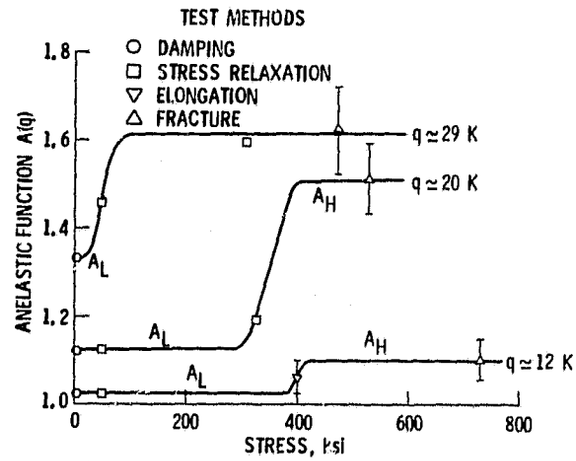

Figure 2. - The effects of stress on the anelastic strain function for as-produced boron fibers.

CS-80-929

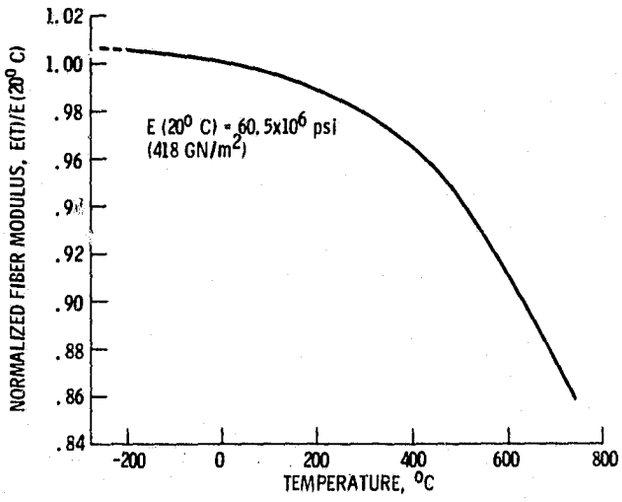

Figure 3. - The normalized axial Young's modulus of boron fibers.

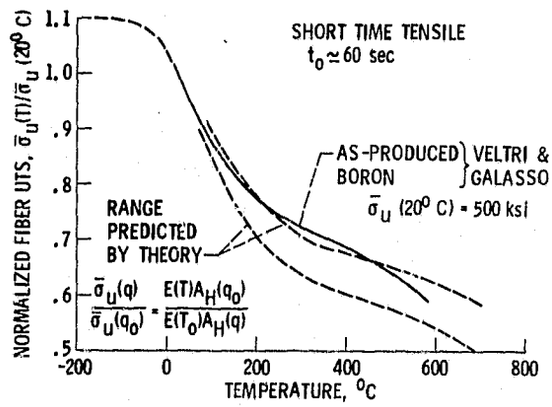

Figure 4. - The normalized ultimate tensile strength of as-produced boron fibers.

CS-80-930

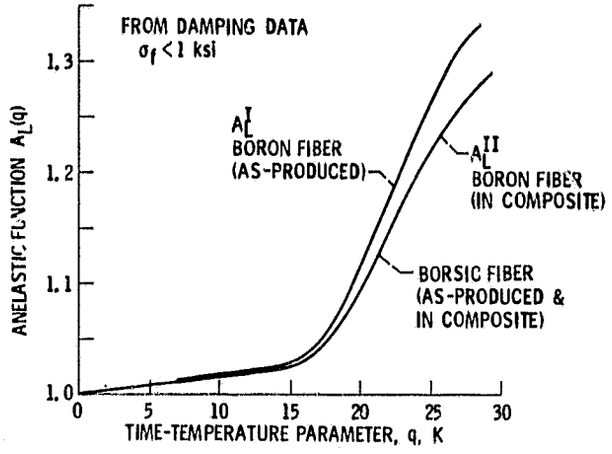

Figure 5. - The effects of composite fabrication and SiC coating on the low-stress anelastic strain function for as-produced boron fibers.

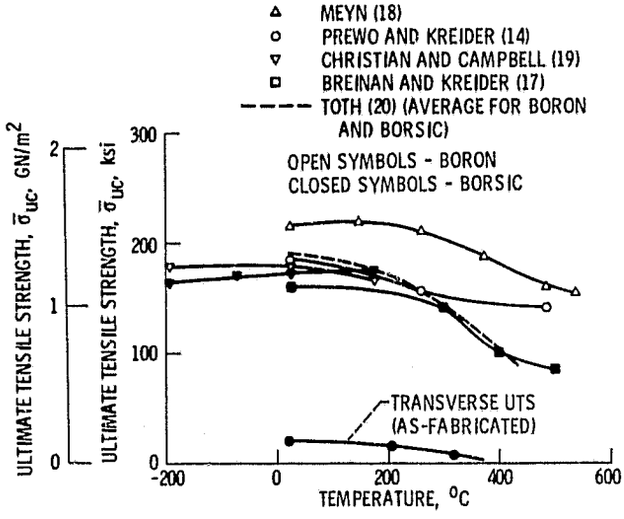

Figure 6. - The ultimate tensile strength of B/6061 Al composites.

CS-80-931

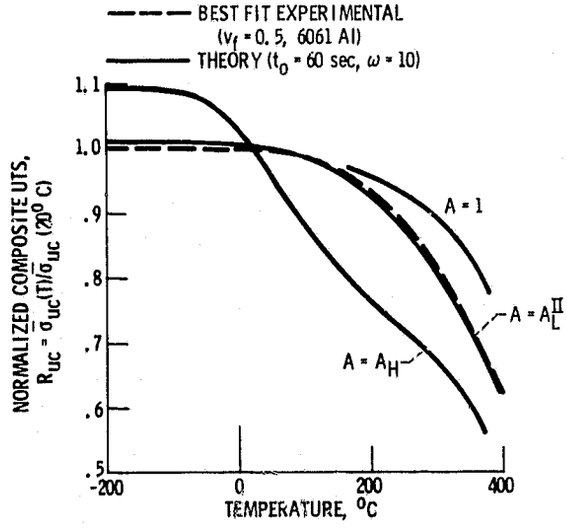

Figure 7. - The normalized ultimate tensile strength of B/6061 Al composites.